Ecole Polytechnique Fédérale de Lausanne
Institut de Théorie des Phénomènes Physiques
Laboratoire de Physique des Particules et Cosmologie

Master Project

On the Analytic Continuation of Field Configurations in Classical Field Theories

Abstract

We develop and test a framework to compute numerically the analytic continuation of some instanton solutions of non linear field equations. The holomorphic nature of the solutions enable us to treat the analytic continuation as an initial value problem, which can be integrated using standard numerical procedures avaliable for Cauchy problems.

Thomas Foetisch, January 20, 2012

This work was achieved under the supervision of:

Prof. Mikhail Shaposhnikov
Ph.D. Alexander Monin

This page was intentionally left blank.

Contents

This page was intentionally left blank.

1 Introduction

Solitons and instantons are particular solutions which arise in non-linear field theories. An instanton is a solution of the euclidian equations of motions which is localized in space and time, whereas solitons are stable solutions of the field equations with an energy density localized in space.

The instanton is an important element of many calculations in field theories. As a simple example, instantons can be used to compute the semi-classical transition amplitude between two states:

$$\left\langle x_f \middle| e^{-HT/\hbar} \middle| x_i \right\rangle = \int \mathcal{D}[x] e^{-S/\hbar} = \sqrt{\frac{\omega}{\pi\hbar}} e^{-\omega T/2} \frac{1}{2} \left[e^{ke^{-S_0\hbar}T} \mp e^{-ke^{-S_0\hbar}T} \right]$$

where x_f and x_i are two vacua, or false vacua, and S_0 the classical action of the instanton. An extensive discussion on the use of instanton is provided by S. Coleman [1]. Tunnelling probabilities may also be obtained.

The situations where the solution to the field equation can be expressed in terms of elementary function are exceptional, and arise only in the simplest theories. From this point of view, obtaining the analytic continuation is not a trivial question.

In this project, we will develop a framework to compute numerically this analytic continuation, provided that a numerical solution of the field equations is already available.

We will first check the features and the properties of the procedure on a set of test cases, for which solutions are already known. We will eventually compute the numerical analytic continuation of the 't Hooft–Polyakov monopole in the Georgi–Glashow model, as well as a vortex in a $(2+1)$ dimensional Yang-Mills theory with $U(1)$ gauge symmetry.

2 Numerical Scheme

In this section, we develop the framework which will allow us to compute numerically the analytic continuation of an arbitrary function. Let

$$\vec{f} : x \in I \subset \mathbb{R} \mapsto \vec{f}(x) \in \mathbb{R}^n \tag{1}$$

be a real-valued function, defined by a set of n differential equations

$$\frac{\mathrm{d}\vec{f}}{\mathrm{d}x} = \vec{F}(\vec{f}(x), x) \tag{2}$$

with n initial or boundary conditions which define univocally $\vec{f}$. Then it is possible, using the Cauchy-Riemann equations to define a new set of differential equations with initial values, which describe the continuation of the function f to the complex plane.

We now assume that the coordinate x is an element of $\mathbb{C}$: $x \to z = x+iy$, as well as the function $\vec{f}$ itself:

$$\vec{f}(x) \to \vec{f}(z) = \vec{f}_R(z) + i\vec{f}_I(z) \tag{3}$$

with f_R and f_I being the real and imaginary parts of $\vec{f}$. Derivative with respect to x must be changed to:

$$\frac{\mathrm{d}\vec{f}}{\mathrm{d}x} \to \frac{\mathrm{d}\vec{f}}{\mathrm{d}z} \equiv \partial_x f_R(x+iy) + i\partial_x f_I(x+iy), \tag{4}$$

and the right hand side of (2) is completed by an imaginary part as well:

$$\vec{F}(\vec{f}(x), x) \to \vec{F}_R(\vec{f}(z), z) + i\vec{F}_I(\vec{f}(z), z). \tag{5}$$

The new system now reads:

$$\partial_x f_R(x+iy) + i\partial_x f_I(x+iy) = \vec{F}_R(\vec{f}(z), z) + i\vec{F}_I(\vec{f}(z), z), \tag{6}$$

$$\Rightarrow \begin{cases} \partial_x f_R(x+iy) = \vec{F}_R(\vec{f}(z), z), \\ \partial_x f_I(x+iy) = \vec{F}_I(\vec{f}(z), z). \end{cases} \tag{7}$$

Assuming that f is analytic, the Cauchy-Riemann equations:

$$\begin{cases} \partial_x f_R = \partial_y f_I, \\ \partial_x f_R = -\partial_x f_I, \end{cases} \tag{8}$$

provide a relationship between the derivative of the real and imaginary parts. These equation allow to rewrite the system (7) in terms of the partial derivatives with respect to the imaginary coordinate:

$$\begin{aligned} \partial_y f_I(x+iy) &= \vec{F}_R(\vec{f}(z), z), \\ -\partial_y f_R(x+iy) &= \vec{F}_I(\vec{f}(z), z). \end{aligned} \tag{9}$$

For $f(z)$ to be an analytic continuation of $f(x)$, both functions must coincide on the intersection of their domain of definitions, that is, on the real axis:

$$f_R(x+i0) + if_I(x+i0) = f(x), \quad \forall x, \tag{10}$$

$$\Rightarrow \begin{cases} f_R(x+i0) = f(x) \\ f_I(x+i0) = 0 \end{cases}, \quad \forall x. \tag{11}$$

From this point, we may integrate numerically the system (9) along $y \in [0, \pm\infty)$ to obtain $f(z)$.

But this procedure is not sufficient for the following reasons. First of all, it may happens that the function $f(x)$ is only defined or known on

a subset of the real line $I \subset \mathbb{R}$. In this case, our procedure would only allow us to find its analytic continuation on a subset of the complex plane $\{z = x + iy \mid x \in I\}$. Secondly, it may also happens that the function f is not defined or analytic on a set of points $\{z_1 \equiv x_1 + iy_1, z_2 \equiv x_2 + iy_2, \dots\}$ away from the real axis. In this case, we can only find a numerical solution for the points $\{z = x_i + iy \mid y < y_i\}$, and the solution cannot be computed beyond these points. In practice, we cannot even come arbitrarily close to these point, as the numerical scheme becomes unstable.

We note that the set of points which are not reachable are related to the choice of coordinates to represent the complex numbers. Hence, changing the coordinates system would also change the set of points which is out of reach. Considering different sets of coordinates would eventually allow us to find the function everywhere.

2.1 Polar coordinates

The typical situation that may arise is the following. A function f is defined $\forall x \in \mathbb{R}_+ - \{0\}$, and we are interested in its analytic continuation on the imaginary axis. Choosing a polar coordinate system is therefore convenient, since it would be sufficient to integrate along the polar angle $\theta \in [0, \pm\pi/2]$. Let's define such a coordinate system by:

$$z = x(r,\theta) + iy(r,\theta), \text{ where } \begin{cases} x = r\cos(\theta) \\ y = r\sin(\theta) \end{cases} \tag{12}$$

and the function f in terms of these coordinates:

$$f(z) = f(x(r,\theta) + iy(r,\theta)) \equiv f(r,\theta). \tag{13}$$

And since we need to integrate the function along θ, we need to find the corresponding Cauchy problem for the real and imaginary parts of $f(r,\theta)$.

Using the chain rule, we have:

$$\frac{\partial f_{R,I}}{\partial\theta}(r,\theta) = \frac{\partial f_{R,I}}{\partial x}(x(r,\theta) + iy(r,\theta))\frac{\partial x}{\partial\theta}(r,\theta) \tag{14}$$

$$+ \frac{\partial f_{R,I}}{\partial y}(x(r,\theta) + iy(r,\theta))\frac{\partial y}{\partial\theta}(r,\theta), \tag{15}$$

$$\Rightarrow \begin{cases} \dfrac{\partial f_R}{\partial\theta}(r,\theta) = \dfrac{\partial f_R}{\partial x}(x(r,\theta) + iy(r,\theta))\dfrac{\partial x}{\partial\theta}(r,\theta) \\ \qquad\qquad + \dfrac{\partial f_R}{\partial y}(x(r,\theta) + iy(r,\theta))\dfrac{\partial y}{\partial\theta}(r,\theta), \\ \dfrac{\partial f_I}{\partial\theta}(r,\theta) = \dfrac{\partial f_I}{\partial x}(x(r,\theta) + iy(r,\theta))\dfrac{\partial x}{\partial\theta}(r,\theta) \\ \qquad\qquad + \dfrac{\partial f_I}{\partial y}(x(r,\theta) + iy(r,\theta))\dfrac{\partial y}{\partial\theta}(r,\theta). \end{cases} \tag{16}$$

At this point, we may use the original differential system (7) and (9) to substitute the derivatives of f:

$$\begin{cases} \dfrac{\partial f_R}{\partial \theta}(r,\theta) = & F_R(f(x(r,\theta)+iy(r,\theta)), z(r,\theta))\dfrac{\partial x}{\partial \theta}(r,\theta) \\ & - F_I(f(x(r,\theta)+iy(r,\theta)), z(r,\theta))\dfrac{\partial y}{\partial \theta}(r,\theta), \\ \dfrac{\partial f_I}{\partial \theta}(r,\theta) = & F_I(f(x(r,\theta)+iy(r,\theta)), z(r,\theta))\dfrac{\partial x}{\partial \theta}(r,\theta) \\ & + F_R(f(x(r,\theta)+iy(r,\theta)), z(r,\theta))\dfrac{\partial y}{\partial \theta}(r,\theta), \end{cases} \tag{17}$$

which can be expressed in the more compact form:

$$\begin{bmatrix} \partial_\theta f_R(r,\theta) \\ \partial_\theta f_I(r,\theta) \end{bmatrix} = \begin{bmatrix} \partial_\theta x(r,\theta) & -\partial_\theta y(r,\theta) \\ \partial_\theta y(r,\theta) & \partial_\theta x(r,\theta) \end{bmatrix} \cdot \begin{bmatrix} F_R(f(z(r,\theta)), z(r,\theta)) \\ F_I(f(z(r,\theta)), z(r,\theta)) \end{bmatrix}. \tag{18}$$

This last expression is valid for any change of coordinates, since we didn't used any special properties of polar coordinates.

Eventually, the polar coordinates leads to the following differential system:

$$\begin{bmatrix} \partial_\theta f_R(r,\theta) \\ \partial_\theta f_I(r,\theta) \end{bmatrix} = -r \begin{bmatrix} \sin(\theta) & \cos(\theta) \\ -\cos(\theta) & \sin(\theta) \end{bmatrix} \cdot \begin{bmatrix} F_R(f(z(r,\theta)), z(r,\theta)) \\ F_I(f(z(r,\theta)), z(r,\theta)) \end{bmatrix}. \tag{19}$$

The initial conditions are given by:

$$\begin{cases} f_R(r,\theta=0) = f_R(r+0i) = f(r) \\ f_I(r,\theta=0) = f_I(r+0i) = 0 \end{cases} \quad \forall r > 0, \tag{20}$$

where $f(r)$ is the solution of the problem on the real axis.

2.2 Vortex and Monopole solutions

A prior condition to use our procedure to compute the analytic continuation of a function to the complex plane is to know the function on the real axis. For the vortex and the monopole, this requires to solve a system of two non linear differential equations with boundary conditions at the origin and infinity. give a brief descriptions of the theories. A more detailed discussion can be found in [2] and [3].

2.2.1 The Vortex in $(2+1)$ dimensions

Let $\mathcal{L}$ be the Lagrangian of a field theory with $U(1)$ gauge symmetry in $(2+1)$ dimensions:

$$\mathcal{L} = -\frac{1}{4}F_{\mu\nu}^2 + (D_\mu\phi)^*(D_\mu\phi) - \frac{\lambda}{2}(\phi^*\phi - v^2)^2. \tag{21}$$

Under the condition of finiteness of the energy functional, the most general static spherically symmetric ansatz can be written as:

$$A_i(r,\theta) = -\frac{1}{er}\varepsilon_{ij}n_j A(r),\ A_0 = 0, \tag{22}$$

$$\phi(r,\theta) = ve^{i\theta}F(r), \tag{23}$$

with the following asymptotics for the two functions A and F:

$$A(0) = F(0) = 0, \tag{24}$$

$$\lim_{r\to\infty} A(r) = \lim_{r\to\infty} F(r) = 1. \tag{25}$$

Substitution of this ansatz into the equations of motions leads to the two independent second order differential equations:

$$-\frac{\mathrm{d}}{\mathrm{d}r}\left(\frac{1}{r}\frac{\mathrm{d}A}{\mathrm{d}r}\right) - 2e^2v^2\frac{F^2(1-A)}{r} = 0, \tag{26}$$

$$-\frac{\mathrm{d}}{\mathrm{d}r}\left(r\frac{\mathrm{d}F}{\mathrm{d}r}\right) + \lambda v^2 rF(F^2-1) + \frac{F(1-A)^2}{r} = 0. \tag{27}$$

There exist no expression of the solution in terms of elementary functions for this problem, thus we are forced to use numerical tools to find an approximation. The numerical techniques available to solve such boundary value problems fall into two main categories.

The first uses a finite element method approach to approximate the derivatives of the functions, reducing the problem to finding zeros of a set of non linear equations. A Newton-Raphson iteration is then used to find a numerical solution to the system.

The second category, generally called shooting method, takes advantage of all the well-developed techniques available to tackle differential initial value problems, by considering the the boundary values at one extremity of the interval as a function of the boundary values at the other extremity. We then need to find the right initial condition such that the solution satisfies the both boundary conditions.

This last method fails in a number of situations, including the case of the vortex, especially when the equations are highly non linear, and tends to develop exponentially growing modes. Careful modification of these methods must be considered in these situations.

For simplicity, a finite elements method have been used to find approximations of the vortex and the monopole, and have shown fast convergence to the solution, even when the initial point of the Newton-Raphson iteration is far from the solution. Details of the computations and the equations used are presented for the interested reader in appendix B. The code was implemented in the C++ language, with the use of the Lapack routines for some linear algebra related operations, such as matrix inversion.

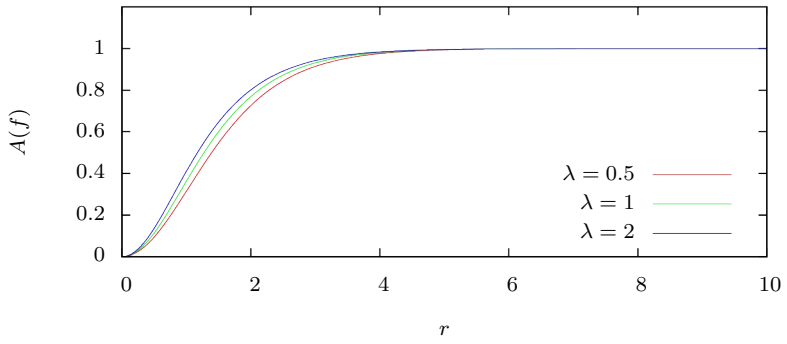

Figure 1: *Profile of the function $A(r)$ for a set of 3 value for the λ coupling constant. A numerical approximation of the function is obtained with a discretization of the interval $[0, 10]$ into $N = 400$ points. The BPS limit correspond to the green curve.*

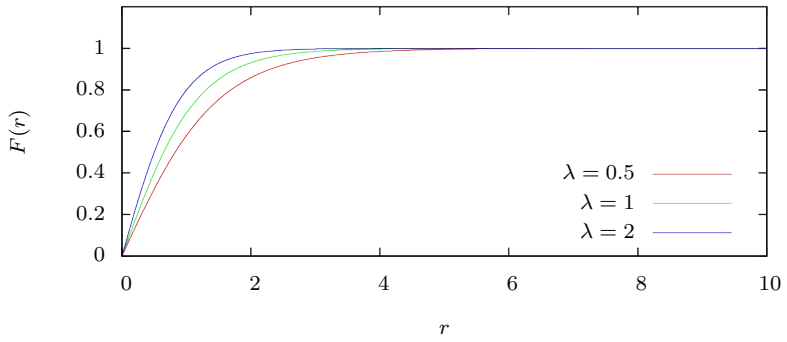

Figure 2: *Profile of the function $F(r)$ for a set of 3 value for the λ coupling constant. A numerical approximation of the function is obtained with a discretization of the interval $[0, 10]$ into $N = 400$ points. The BPS limit correspond to the green curve.*

Fig. 1 and 2 show the profile of the two functions A and F for different values of the Higgs field coupling constant λ. The situation where $\lambda = 1$ correspond to the Bogomol'nyi-Prasad-Sommerfield limit (BPS limit).

2.2.2 The Monopole in $(3+1)$ dimensions

Let $\mathcal{L}$ be the Lagrangian of a $SU(2)$ gauge field theory, usually attributed to Georgi and Glashow:

$$\mathcal{L} = -\frac{1}{4}F^a_{\mu\nu}F^a_{\mu\nu} + \frac{1}{2}(D_\mu\phi)^a(D_\mu\phi)^a - \frac{\lambda}{4}(\phi^a\phi^a - v^2)^2, \tag{28}$$

where A_μ and ϕ belongs to the $SU(2)$ algebra. t'Hooft and Polyakov have shown that there exists static solution with finite energy. Indeed, the most general static spherically symmetric solution can be written as:

$$\phi^a(\vec{r}) = n^a v h(r), \tag{29}$$

$$A^a_i(\vec{r}) = \frac{1}{gr}\varepsilon^{aij}n^j f(r), \tag{30}$$

where the finiteness of the energy imposes the following asymptotics for the two functions f and h:

$$f(0) = h(0) = 0, \tag{31}$$

$$\lim_{r\to\infty} f(r) = \lim_{r\to\infty} h(r) = 1. \tag{32}$$

Substitution of this ansatz into the equations of motions leads to the following system of second order differential equations:

$$r(rh'' + 2h') - 2h(f-1)^2 + \lambda v^2 r^2 h(1-h^2) = 0, \tag{33}$$

$$r^2 f'' = f(f-1)(f-2) + g^2 v^2 r^2 h^2 (f-1). \tag{34}$$

It is convenient to perform the following change of field definitions:

$$M(r) := rh(r) \Rightarrow M''(r) = rh''(r) + 2h'(r), \tag{35}$$

$$N(r) := 1 - f(r) \Rightarrow N''(r) = f''(r). \tag{36}$$

And the equations in terms of these new fields become:

$$r^2 M''(r) = 2M(r)N(r)^2 + \lambda v^2 M(r)(M(r)^2 - r^2), \tag{37}$$

$$r^2 N''(r) = M(r)(M(r)^2 - 1) + gv^2 N(r)^2 M(r). \tag{38}$$

These equations are the ones that where originally derived by 't Hooft and Polyakov. This latter form was used in the numerical integration. As previously mentioned, a finite element method was used in order to find a numerical solution.

The results of the integration of functions M and N is presented on Fig. 3 and 4, for a set of three values of the Higgs coupling constant λ.

The situation where $\lambda = 0$ correspond to the BPS limit, and is special in the sense that the solution can be expressed in terms of elementary functions:

$$M(r) = \frac{r}{\tanh(r)} - 1 \quad ; \quad N(r) = \frac{r}{\sinh(r)}. \tag{39}$$

This situation is very valuable, since it gives a mean of checking the convergence of the analytic continuation in a very non trivial situation.

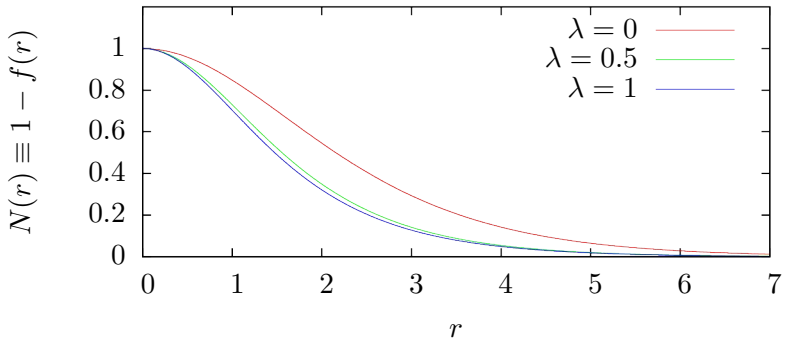

Figure 3: *Profile of the function $N(r)$ for a set of 3 value for the λ coupling constant. A numerical approximation of the function is obtained with a discretization of the interval $[0, 10]$ into $N = 400$ points. The BPS limit correspond to the red curve.*

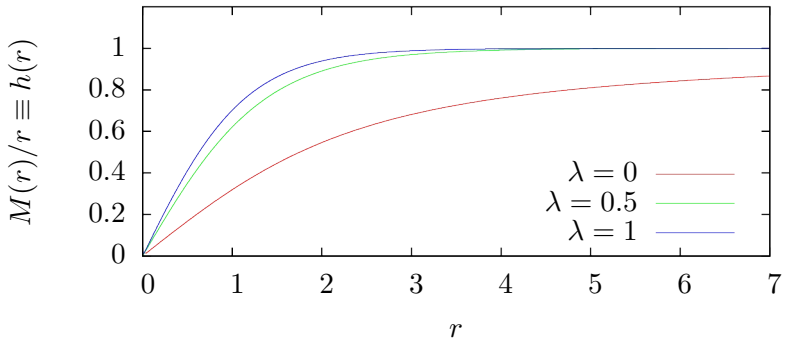

Figure 4: *Profile of the function $M(r)/r$ for a set of 3 value for the λ coupling constant. We note that the asymptotic behaviour of the BPS limit case is note exponentially reaching 1 (red curve). In order to obtain a reasonable approximation, the boundary condition $M(r)/r = 1$ must be imposed for a large radius. We used a discretization of the interval [0,100] into $N = 3000$ points.*

3 Validity tests

Before using the procedure proposed in paragraph 2, we need to get convinced of its validity. For this purpose, we used a set of test case, where the solution is already known, and a closed form expression is available. One of the test cases is derived from a Sine-Gordon field equations.

The method proposed attempt to compute the value of a function in

some region of the complex plane, provided that we have a set of differential equations which describe the function, and its values known on a subset of the real axis.

3.1 Riemann sheet: the square root

We know try to find the analytic continuation of the square root on the complex plane:

$$f(x) := \sqrt{x}. \tag{40}$$

The first step is to find a differential equation. This is easily achieved:

$$f'(x) = \frac{1}{2}x^{-1/2} = \frac{1}{2\sqrt{x}} = \frac{1}{2f(x)}, \tag{41}$$

$$\Rightarrow f'(x) = \frac{1}{2f(x)}. \tag{42}$$

If we know promote the function f to be a complex number, using the Cauchy-Riemann equations (8), we obtain the following system of differential equations:

$$\partial_x f_R(z) + i\partial_x f_I(z) = \frac{1}{2(f_R(z) + if_I(z))}, \tag{43}$$

$$\Rightarrow \begin{cases} \partial_y f_I(z) = \dfrac{f_R(z)}{2(f_R^2(z) + f_I^2(z))}, \\ -\partial_y f_R(z) = -\dfrac{f_I(z)}{2(f_R^2(z) + f_I^2(z))}. \end{cases} \tag{44}$$

with the initial conditions:

$$f_R(x + i0) = \sqrt{x}, \tag{45}$$

$$f_I(x + i0) = 0. \tag{46}$$

We note that the function $-\sqrt{x}$ is also a solution of (42). Obtaining the square root or its opposite is related to the choice of the initial conditions of the Cauchy problem.

The result of the integration of the Cauchy problem is presented on Fig. 5, for $\theta \in [0, 4\pi]$. It is interesting to note that this procedure gives an access, at least in this case, to the complete Riemann manifold of the square root. The first 2π of the integration gives the upper sheet of the manifold, and the last 2π gives the lower sheet.

The procedure is valid for this simple function, and converges to the continuation of the square root defined by:

$$\sqrt{z} = \sqrt{\frac{|z| + \Re z}{2}} \pm i\sqrt{\frac{|z| - \Re z}{2}}. \tag{47}$$

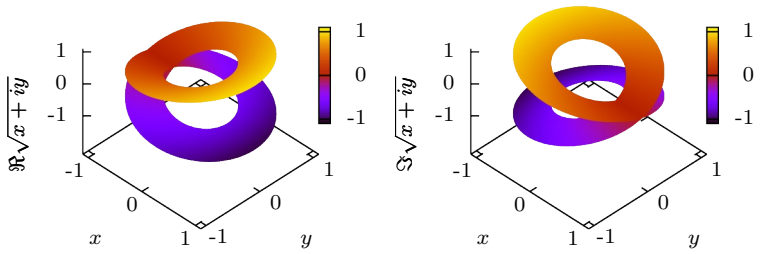

Figure 5: *Real (left) and imaginary (right) values of the analytic continuation of the square root function. The integration starts on the real axis, and ends exactly at the same place after two (4π) complete revolutions around the origin. The integration was performed using a polar coordinate system.*

3.2 The logarithm

It is now interesting to consider a function which presents a different type of singularity at the origin. The natural logarithm is a good candidate:

$$f(x) := \log(x). \tag{48}$$

The corresponding differential equation is easily found as previously:

$$f'(x) = \frac{1}{x} = \exp(-\log(x)) = \exp(-f(x)). \tag{49}$$

Promoting the f function to be a complex number gives the following set of equations:

$$\begin{cases} \partial_y f_I(z) = \exp(-f_R(z))\cos(f_I), \\ -\partial_y f_R(z) = -\exp(-f_R(z))\sin(f_I), \end{cases} \tag{50}$$

with the initial condition:

$$\begin{cases} f_R(x+i0) = \log(x), \\ f_I(x+i0) = 0. \end{cases} \tag{51}$$

The result of the integration is presented on Fig. 6. As for the square root, we have access to the complete Riemann manifold. In these case, no particular branch cut is chosen or imposed by the procedure. In this situation, in the range $\theta \in [-\pi, \pi]$ the numerical solution converges to

$$\log(z) = \log(|z|) + i \arctan\left(\frac{y}{x}\right). \tag{52}$$

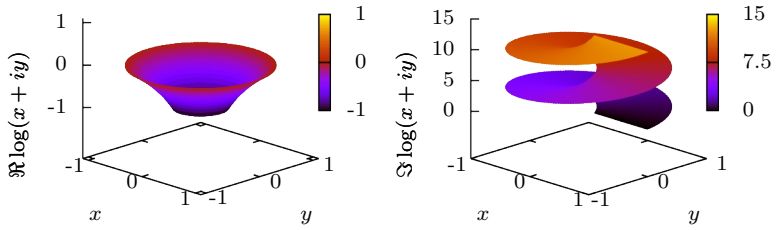

Figure 6: *Real (left) and imaginary (right) values of the analytic continuation of the logarithm function. The integration was performed using a polar coordinate system. The integration starts on the real axis. The real component of* $\log(z)$ *for a given* $|z|$*. The imaginary part increase linearly with respect to* θ*, increasing by* 2π *at each revolution around the origin.*

3.3 Quantum pendulum in gravitation

The last test case is less arbitrary, and in a sense related to the real problems to which we will eventually apply our analytic continuation procedure.

Let's consider a pendulum in the field of gravity, which is described by the Lagrangian:

$$\mathcal{L} = \frac{1}{2}\dot{\phi}^2 - (\cos(\phi) - 1). \tag{53}$$

We are interested in the instanton solution of the theory. The Hamiltonian is given by:

$$h(t) = \frac{1}{2}\dot{\phi}^2 + \cos(\phi). \tag{54}$$

It does not directly depends upon time, thus the energy is conserved. An instanton correspond to a trajectory which start at $\phi = 0$ and ends at $\phi = 2\pi$:

$$\lim_{t\to-\infty} \phi(t) = 0 \ ; \ \lim_{t\to\infty} \phi(t) = 2\pi. \tag{55}$$

In this situation, assuming that $\lim_{t\to-\infty} \dot{\phi} = 0$ the Hamiltonian gives:

$$h(t) = h = 0 = \frac{1}{2}\dot{\phi}^2 + \cos(\phi) - 1. \tag{56}$$

Integrating by separation of variables gives the solution for the time dependence of the instanton:

$$\phi(t) = 4\arctan(\exp(t)). \tag{57}$$

The analytic continuation of this solution was computed using the second order equation of motion:

$$\ddot{\phi}(t) = \sin(\phi(t)), \tag{58}$$

which must be recast into a first order equation, introducing a new variable:

$$\dot{\phi}(t) = \omega(t), \tag{59}$$
$$\dot{\omega}(t) = \sin(\phi(t)), \tag{60}$$

and the system to be integrated reads:

$$\begin{cases} \partial_y \phi_I = \omega_R, \\ \partial_y \omega_I = \sin(\phi_R)\cosh(\phi_I), \\ -\partial_y \phi_R = \omega_I, \\ -\partial_y \omega_R = \cos(\phi_R)\sinh(\phi_I), \end{cases} \tag{61}$$

with initial conditions at $(t, y = 0)$:

$$\begin{cases} \phi_I(t + i0) = 0, \\ \omega_I(t + i0) = 0, \\ \phi_R(t + i0) = 4\arctan(\exp(t)), \\ \omega_R(t + i0) = \dfrac{4\exp(t)}{1 + \exp(2t)}. \end{cases} \tag{62}$$

A qualitative view of the numerical results are provided by Fig. 7, only for the first quadrant of the complex plane (which corresponds to the integration along the θ polar coordinate from 0 to $\pi/2$). We recognize on the x axis (real axis) of the real part of the analytic continuation, the profile of the instanton. Moreover, we clearly distinguish singularities regularly spaced on the imaginary axis. It is exactly what is expected by the analytic continuation of the function $4\arctan(\exp(z))$.

Fig. 8 and 9 show the real and imaginary parts of the solution. We clearly distinguish the singularities on the imaginary axis. There are infinitely many of them, located at $(2n + 1)\pi/2, n = 0, 1, \ldots$. We also notice the formation of a discontinuity after each one of them on the real part of the function.

This example demonstrates one interesting feature of the procedure of analytic continuation. It can be shown that the singularities on the imaginary axis are of the same type as the singularity at the origin for the logarithm. The choice of a coordinate system imposes naturally a set of coordinate paths, and the result of the integration along these paths depends on the singularities which lie on each side of the paths.

For this reason, the branch cuts appear naturally along the coordinate lines.

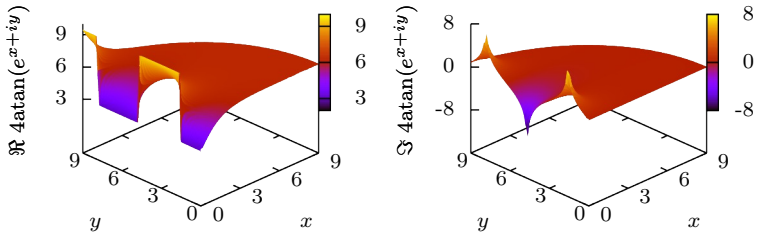

Figure 7: *Real (left) and imaginary (right) parts of the analytic continuation of the solution. We distinguish the first 3 singularities on the positive imaginary axis, at $i\pi/2$, $i3\pi/2$, $i5\pi/2$. A polar coordinate system was used for the integration.*

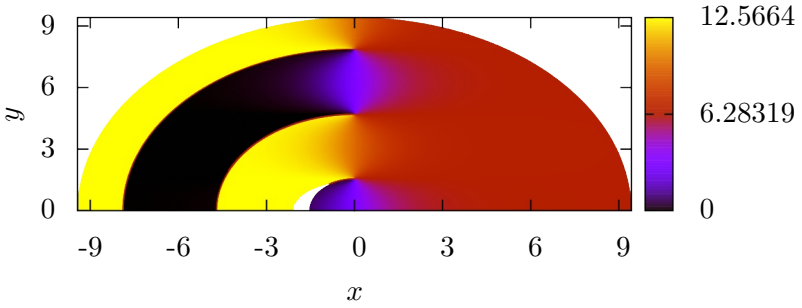

Figure 8: *Real part of the solution in the positive imaginary half plane. The solution is the same in the negative half plane. We clearly see the branch cut starting from each singularity.*

Finally, Fig. 10 shows the behaviour of the function in the vicinity of a singularity. The difference of the value of the function along two paths is represented. The first path passes at a distance Δ below the first singularity on the positive imaginary axis, and the second path passes at a distance Δ above the same singularity. Ideally $\Delta \to 0$ but it is numerically not feasible. We notice that away from the singularity, the size of the step is essentially constant, reaching 4π for $\theta \geq \pi/2$. This is a consequence of Cauchy's theorem, and it is accurately reproduced here.

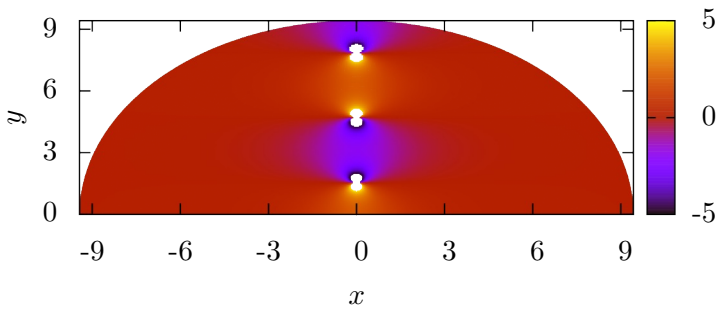

Figure 9: *Imaginary part of the solution in the positive imaginary half plane.*

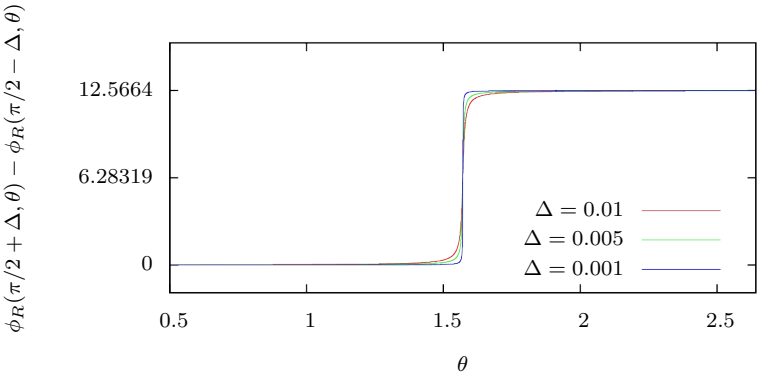

Figure 10: *Difference of the real part of the solution for two paths separated by a distance of* 2Δ*. Once the two paths pass aside of the first singularity, a step of* 4π *appear. Away from the singularity, the step remains constant.*

4 Application to the Vortex in $(2+1)$ dimensions

We now use the same procedure to compute the numerical analytic continuation of the Vortex, which arises in $(2+1)$ dimensional Yang-Mills theory with $U(1)$ gauge symmetry.

The Lagrangian and the ansatz considered have been introduces in section 2.2.1. We now build the Cauchy problem related to the analytic continuation of the vortex.

We first recast the second order differential equation system into a first

order system: we define $B(r) = A'(r)$ and $G(r) = F'(r)$, which leads to

$$\frac{\mathrm{d}}{\mathrm{d}r}A = B(r), \tag{63}$$
$$\frac{\mathrm{d}}{\mathrm{d}r}B = \frac{1}{r}B(r) - 2e^2v^2F(r)^2(1 - A(r)), \tag{64}$$
$$\frac{\mathrm{d}}{\mathrm{d}r}F = G(r), \tag{65}$$
$$\frac{\mathrm{d}}{\mathrm{d}r}G = -\frac{1}{r}G(r) + \lambda v^2(F(r)^2 - 1)F(r) + \frac{F(r)(A(r) - 1)^2}{r^2}. \tag{66}$$

Promoting all the functions A, B, F, G to the complex field, as well as $r \to z = r + iy$ and following the same procedure as previously, the Cauchy problem writes:

$$\partial_y A_I = B_R, \tag{67}$$
$$-\partial_y A_R = B_I, \tag{68}$$
$$\partial_y B_I = \Re\left[\frac{B_R + iB_I}{z} - 2e^2v^2(F_R + iF_I)^2(1 - (A_R + iA_I))\right], \tag{69}$$
$$-\partial_y B_R = \Im\left[\frac{B_R + iB_I}{z} - 2e^2v^2(F_R + iF_I)^2(1 - (A_R + iA_I))\right], \tag{70}$$
$$\partial_y F_I = G_R, \tag{71}$$
$$-\partial_y F_R = G_I, \tag{72}$$
$$\partial_y G_I = \Re\left[-\frac{G_R + iG_I}{z} + \lambda v^2((F_R + iF_I)^2 - 1)(F_R + iF_I)\right. \tag{73}$$
$$\left. + \frac{(F_R + iF_I)(A_R + iA_I - 1)^2}{z^2}\right], \tag{74}$$
$$-\partial_y G_R = \Im\left[-\frac{G_R + iG_I}{z} + \lambda v^2((F_R + iF_I)^2 - 1)(F_R + iF_I)\right. \tag{75}$$
$$\left. + \frac{(F_R + iF_I)(A_R + iA_I - 1)^2}{z^2}\right]. \tag{76}$$
$$\tag{77}$$

The actual computation of the real and imaginary parts of these last expression is clearly tedious and uninteresting. Therefore the job is left to the numerical implementation.

The initial conditions of this Cauchy problem require the values of the the functions A and F, as well as their derivative. Both of them are obtained numerically for a set of points uniformly distributed on the real axis, between 0 and $R = 10$. Each of these points is then used as an initial condition for the analytic continuation.

The initial conditions writes:

$$A_R(r + i0) = A(r), \tag{78}$$
$$B_R(r + i0) = \frac{\mathrm{d}}{\mathrm{d}r}A(r), \tag{79}$$
$$F_R(r + i0) = F(r), \tag{80}$$
$$G_R(r + i0) = \frac{\mathrm{d}}{\mathrm{d}r}F(r), \tag{81}$$
$$A_I(r + i0) = 0, \tag{82}$$
$$B_I(r + i0) = 0, \tag{83}$$
$$F_I(r + i0) = 0, \tag{84}$$
$$G_I(r + i0) = 0. \tag{85}$$
$$\tag{86}$$

It is important to notice that the only coordinate left by the spherical symmetry is the radius r, which is not equivalent to a cartesian coordinate x or y, despite the fact that they share the same numerical value in some situations.

As a consequence, a path in x coordinate starting at $-\infty$ and ending at $+\infty$ corresponds, in terms of r coordinate to a path starting and ending at $+\infty$.

Then, the Wick rotation of such a path brings it to the imaginary axis, without the need to go to the negative real half of the complex plane. An illustration of the Wick's rotation is shown on Fig. 11.

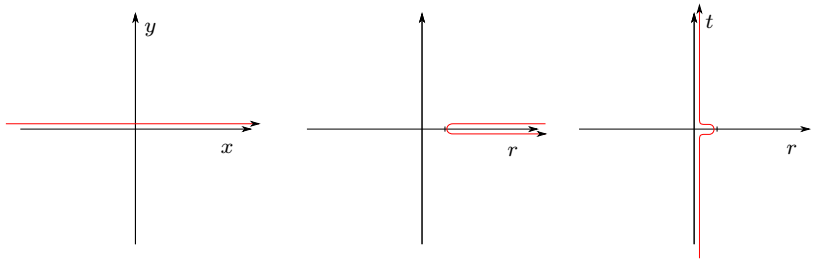

Figure 11: *The choice of the radius r as the coordinate has implications on the Wick rotation of the integration path in the complex plane. The path starting from $-\infty$ to $+\infty$ for the cartesian coordinate x is wrapped in r-space on $\mathbb{R}_+$. The Wick rotation then bring the wrapped path to the imaginary axis, without the need to go to the negative imaginary half plane.*

It is therefore sufficient to restrict the computation of the analytic continuation to the positive real half of the complex plane. We only integrate a little further to make the localization of the singularities easier.

We have computed the analytic continuation of the vortex only in the BPS limit case ($\lambda = 1$). The result for the real and imaginary parts of functions $A(z)$ and $F(z)$ is shown on Fig. 12–15.

4.1 Numerical analytic continuation in the BPS limit

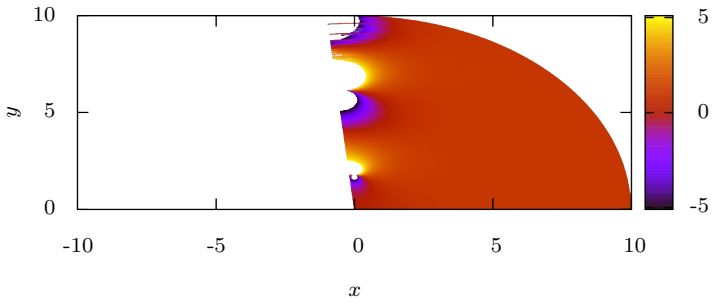

Figure 12: *Real part of the function $A(z)$. The function is even under conjugation: $\Re A(z) = \Re A(\bar{z})$. The singularity which is closest to the origin is on the imaginary axis ($z_0 \approx 0 + 1.78i$). The second one is slightly shifted to the negative real half plane ($z_0 \approx -0.4 + 6.1i$).*

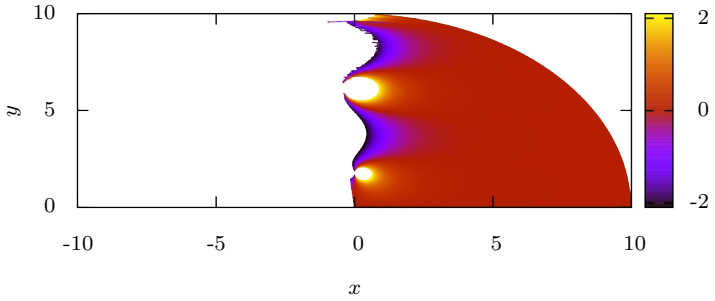

Figure 13: *Imaginary part of the function $A(z)$. The function is odd under conjugation: $\Im A(z) = -\Im A(\bar{z})$.*

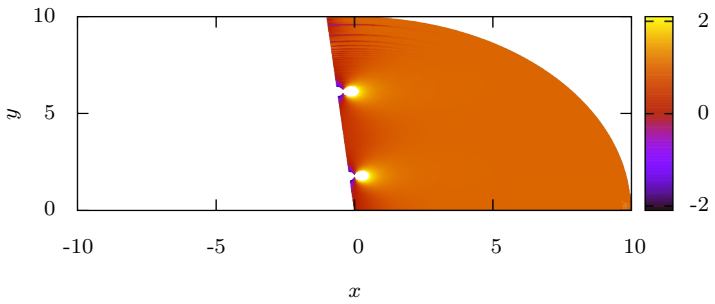

Figure 14: *Real part of the function $F(z)$. The function is even under conjugation: $\Re F(z) = \Re F(\bar{z})$. The locations of the singularities are the same as for the function $A(z)$.*

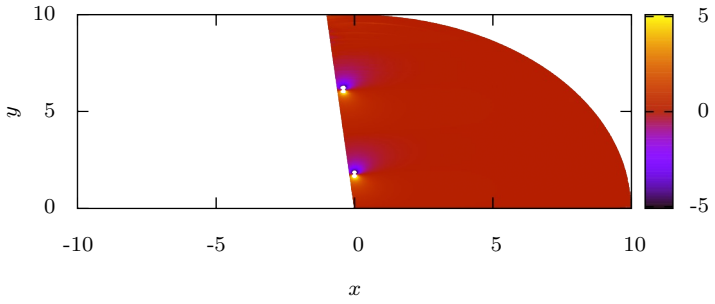

Figure 15: *Imaginary part of the function $F(z)$. The function is odd under conjugation: $\Im F(z) = -\Im F(\bar{z})$.*

We notice two singularities. The first, which is the closest to the origin, lies on the imaginary axis, at least at machine precision. However, the next singularity is off the imaginary axis, and is located on the second quadrant.

The important point is that in positive half of the complex plane, and within the range considered, the analytic continuation of the vortex solution do not show any singularities. This is comforting, since it means that the Wick rotation should be valid and doable in principle.

4.2 Analytic study of the convergence of the Taylor Series

We have now some clues about the existence of a singularity on the imaginary axis. But numerical results are difficult to interpret, and it would be nice

to have an analytic approach to validate this statement.

The idea is to find the Taylor series for the two functions around $z = 0$, and then extract the radius of convergence of these series.

Let N be the order of the Taylor expansions. Using the asymptotics of the two functions A and F, we may write:

$$A(z) = \alpha z^2 + \sum_{i=3}^{N} a_i z^i + O(z^{N+1}), \tag{87}$$

$$F(z) = \beta z + \sum_{i=2}^{N} f_i z^i + O(z^{N+1}). \tag{88}$$

We then substitute these expression into the system of differential equations (26)–(27). These equations must be satisfied at each order in z. Each coefficient of powers of z must cancel, providing a set of equations. α and β are two free parameters which correspond to the two additional initial conditions required to solve a system of 2 second order differential equations. These can be extracted from the numerical approximation of the vortex.

The set of equations has been solved with the help of Mathematica. An estimation of the radius of convergence is presented on Fig. 16. The radius

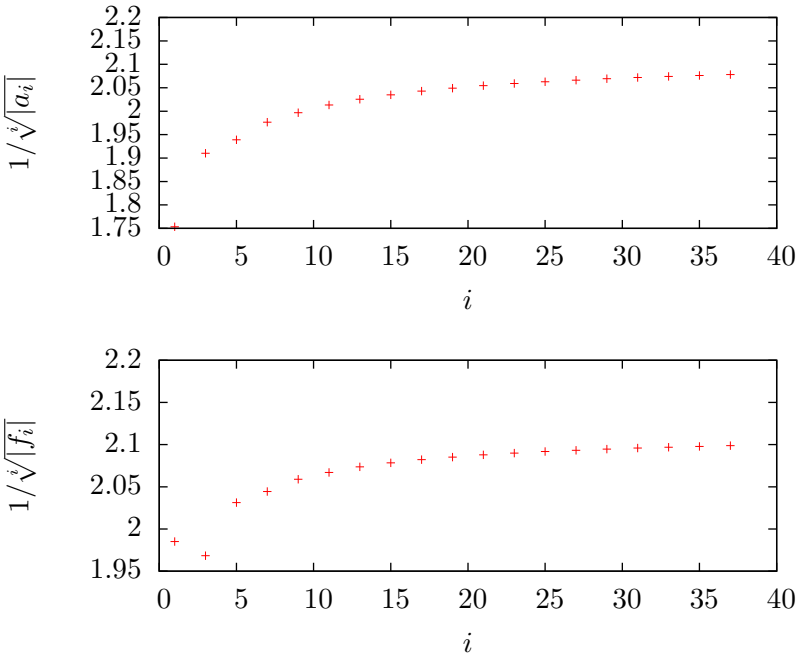

Figure 16: *Radius of convergence computed with the 40 first coefficients of the Taylor series of the function $A(z)$ (top) and $F(z)$ (bottom).*

of convergence of a series $f(x) = \sum_i f_i x^i$ from the general point of view is given by:

$$R = \frac{1}{\limsup_{i\to\infty} \sqrt[i]{|f_i|}}. \tag{89}$$

Using the numerical values of the coefficients, we find the following estimations of the radius of convergence of the series for each functions:

Function $A(z)$	Function $F(z)$
$\frac{1}{\sqrt[40]{\lvert a_{40}\rvert}} \approx 2.1$	$\frac{1}{\sqrt[39]{\lvert f_{39}\rvert}} \approx 2.1$

With a maximal radius of convergence of ~ 2.1, this analysis seems to predict the first singularity further from the origin than what is observed on the numerical simulations. However, with no estimation of the error on these numerical values, no conclusion can be drawn to validate or unvalidate the numerical solution of the vortex.

5 Application to the Monopole in $(3+1)$ dimensions

We now turn to the case of the magnetic monopoles. The Georgi-Glashow model, which is an $SU(2)$ gauge theory, with a potential which allow the Higgs mechanism to take place. The Lagrangian and the ansatz has been presented in section 2.2.2, and we know derive the Cauchy problem which correspond to the analytic continuation of the monopole solution.

Again, the first step is to recast the second order system to a first order system, introducing two new variables:

$$M'(r) = S(r), \tag{90}$$

$$S'(r) = 2\frac{M(r)N(r)^2}{r^2} + \lambda v^2 \frac{M(r)(M(r)^2 - r^2)}{r^2}, \tag{91}$$

$$N'(r) = T(r), \tag{92}$$

$$T'(r) = \frac{M(r)(M(r)^2 - 1)}{r^2} - gv^2 \frac{N(r)^2 M(r)}{r^2}. \tag{93}$$

Again, we promote M, N, S and T as well as the coordinate $r \to z = r + iy$

to the complex field. The Cauchy problem writes:

$$\partial_y M_I = S_R, \tag{94}$$
$$-\partial_y M_R = S_I, \tag{95}$$
$$\partial_y S_I = \Re\left[2\frac{(M_R+iM_I)(N_R+iN_I)^2}{z^2}\right. \tag{96}$$
$$\left. + \lambda v^2 \frac{(M_R+iM_I)((M_R+iM_I)^2-z^2)}{z^2}\right], \tag{97}$$
$$-\partial_y S_R = \Im\left[2\frac{(M_R+iM_I)(N_R+iN_I)^2}{z^2}\right. \tag{98}$$
$$\left. + \lambda v^2 \frac{(M_R+iM_I)((M_R+iM_I)^2-z^2)}{z^2}\right], \tag{99}$$
$$\partial_y N_I = T_R, \tag{100}$$
$$-\partial_y N_R = T_I, \tag{101}$$
$$\partial_y T_I = \Re\left[\frac{(M_R+iM_I)((M_R+iM_I)^2-1)}{z^2}\right. \tag{102}$$
$$\left. - gv^2 \frac{(N_R+iN_I)^2(M_R+iM_I)}{z^2}\right], \tag{103}$$
$$-\partial_y T_R = \Im\left[\frac{(M_R+iM_I)((M_R+iM_I)^2-1)}{z^2}\right. \tag{104}$$
$$\left. - gv^2 \frac{(N_R+iN_I)^2(M_R+iM_I)}{z^2}\right], \tag{105}$$

with the following initial conditions:

$$M_R(r+i0) = M(r), \tag{106}$$
$$S_R(r+i0) = \frac{\mathrm{d}}{\mathrm{d}r}M(r), \tag{107}$$
$$N_R(r+i0) = N(r), \tag{108}$$
$$T_R(r+i0) = \frac{\mathrm{d}}{\mathrm{d}r}N(r), \tag{109}$$
$$M_I(r+i0) = 0, \tag{110}$$
$$S_I(r+i0) = 0, \tag{111}$$
$$N_I(r+i0) = 0, \tag{112}$$
$$T_I(r+i0) = 0, \tag{113}$$
$$\tag{114}$$

Approximations of the values of M and N are obtained, as for the vortex, by numerical means on a discretization of the interval $[0, 10]$.

The analytic continuation of the monopole was computed in two different case. The first is the BPS limit ($\lambda = 0$), and the second with $\lambda = 0.5$.

5.1 Numerical analytic continuation in the BPS limit

This situation is especially useful to check the correctness of the implementation of the numerical scheme, as well its convergence to the solution.

Fig. 17–20 present real and imaginary parts of functions M and N as a result of the numerical integration.

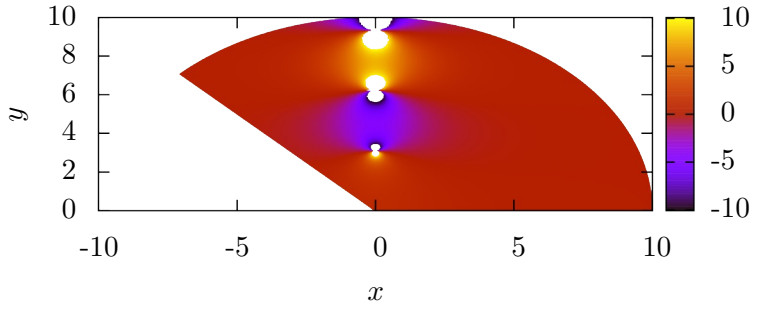

Figure 17: *Real part of the function $N(z)$ in the BPS limit. All the singularities lie on the imaginary axis. The function is even under conjugation:* $\Re N(z) = \Re N(\bar{z})$.

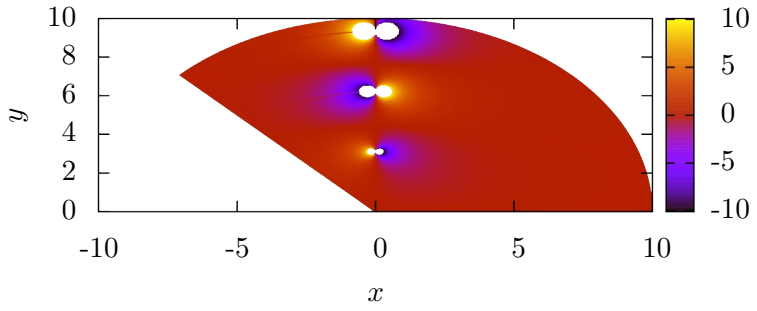

Figure 18: *Imaginary part of the function $N(z)$ in the BPS limit. The function is odd under conjugation:* $\Im N(z) = -\Im N(\bar{z})$.

Beside the fact that the numerical scheme has shown to converge to the solution, the most important feature to notice is that all the singularities lie

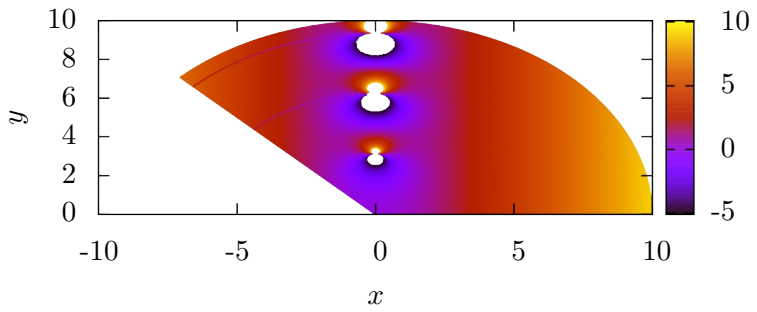

Figure 19: *Real part of the function $M(z)$ (not $M(z)/z$, as on Fig. 3) in the BPS limit. All the singularities lie on the imaginary axis. The function is even under conjugation: $\Re N(z) = \Re N(\bar{z})$.*

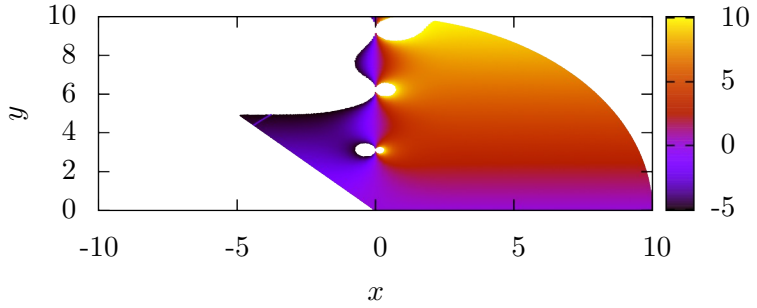

Figure 20: *Imaginary part of the function $N(z)$ in the BPS limit. The function is odd under conjugation: $\Im N(z) = -\Im N(\bar{z})$. The extended white regions correspond to out of range values.*

on the imaginary axis.

The next subsection show the behaviour of the solution when the Higgs coupling constant λ is slightly increased.

5.2 Numerical analytic continuation, $\lambda \neq 0$

In the BPS limit, all the singularities of the functions were lying on the imaginary axis, but it is not the case anymore, as can be seen on Fig. 21–24.

Only the one which is closest to the origin stays on the imaginary axis, and all the other have been shifted to the negative real half complex plane.

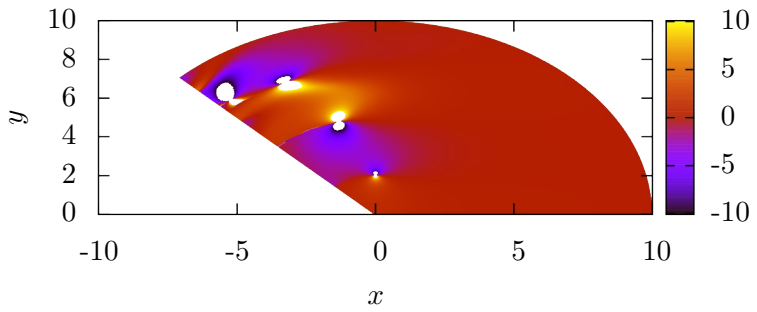

Figure 21: *Real part of the function $N(z)$ with $\lambda = 0.5$. The singularity which is closest to the origin lie on the imaginary axis ($z_0 \approx 0 + 2.05i$). In comparison to the BPS limit, all the other singularities are now shifted to the negative imaginary half plane (coordinates of the second one: $z_0 \approx -1.32 + 4.8i$). The function is even under conjugation: $\Re N(z) = \Re N(\bar{z})$.*

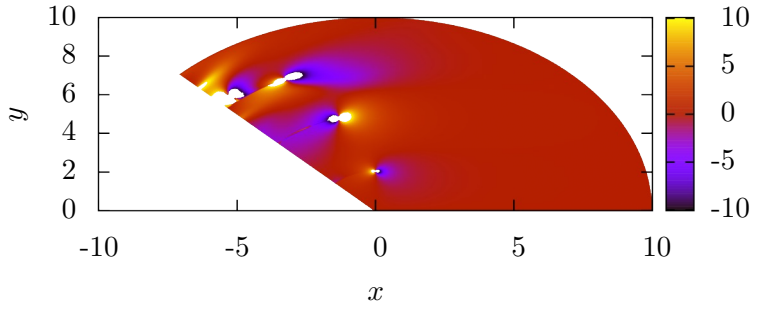

Figure 22: *Imaginary part of the function $N(z)$ with $\lambda = 0.5$. The function is odd under conjugation: $\Im N(z) = -\Im N(\bar{z})$.*

6 Conclusion

We have been able, using our numerical procedure, to find a numerical analytic continuation for a vortex and the 't Hooft–Polyakov monopole in the Georgi–Glashow model. In both case, the solutions showed no singulary in the positive real half of the complex plane, at least in a radius $R = 10$ around the origin. Obtaining the instanton with a Wick rotation of the soliton should therefore be possible. There are still many leads to explore in order to close the subject. First of all, the actual implementation is difficult to generalize to an arbitrary, and its only purpose is as a proof of concept.

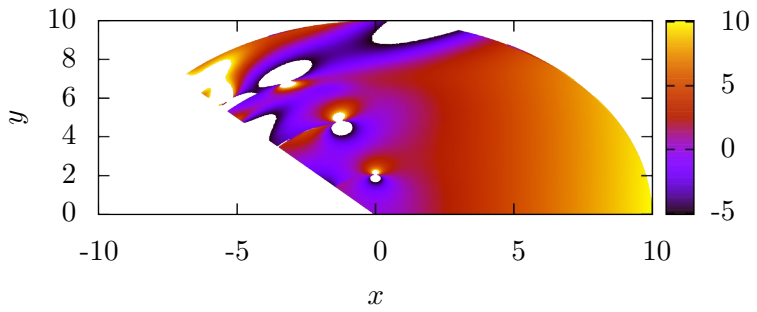

Figure 23: *Real part of the function $M(z)$ (not $M(z)/z$, as on Fig. 3) for $\lambda = 0.5$. The function is even under conjugation: $\Re M(z) = \Re M(\bar{z})$. The extended white regions correspond to out of range values.*

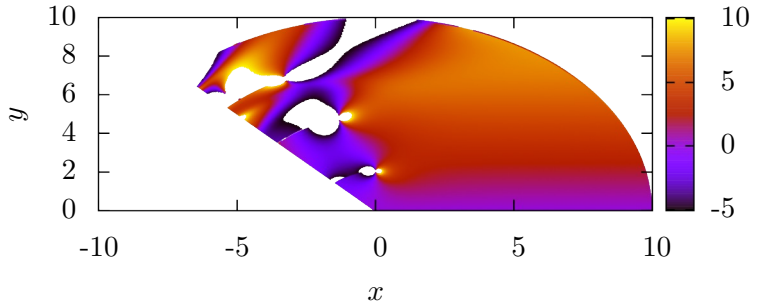

Figure 24: *Imaginary part of the function $M(z)$ for $\lambda = 0.5$. The function is odd under conjugation: $\Im M(z) = -\Im M(\bar{z})$. The extended white regions correspond to out of range values.*

In order to use it in a production environment, it should be rewritten to benefit from all the existing tools that already exist, and that are much more efficient.

The convergence study of the Taylor series has been investigated for the vortex only. But the situation is different for the 't Hooft–Polyakov monopole. The existance of a solution expressed in terms of elementary function in the BPS limit may bring some lights on the convergence properties of the series.

A last feature provided by the numerical analytic continuation has still not been exploited. Using the freedom of the choice of the coordinate system, we could choose a polar coordinate system centered on a singularity, giving

the possibility to obtain the a numerical solution on a closed path around a singularity. Such a numerical solution may allow a deeper inverstigation on the properties of the singularities.

Appendices

A Field equations for Georgi-Glashow model. Monopole solution.

The Lagrangian of the model is given by:

$$\mathcal{L} = -\frac{1}{4}F^a_{\mu\nu}F^{a,\mu\nu} + \frac{1}{2}D_\mu\phi^a D^\mu\phi^a - \frac{\lambda}{4}\left(\phi^a\phi^a - v^2\right), \tag{115}$$

where

$$D_\mu\phi^a \equiv \phi^a{}_{;\mu} = \partial_\mu\phi^a + g\varepsilon^{abc}A^b_\mu\phi^c, \tag{116}$$

$$F^a_{\mu\nu} = \partial_\mu A^a_\nu - \partial_\nu A^a_\mu + g\varepsilon^{abc}A^b_\mu A^c_\nu. \tag{117}$$

By requiring that the first order of the variation of the action around the classical trajectory, we find the following equivalent of the Euler-Lagranges equations for the equation of motion:

$$\frac{\partial\mathcal{L}}{\partial\phi^a} - D_\mu\frac{\mathcal{L}}{\partial\phi^a{}_{;\mu}} = 0, \quad \forall a = 1,2,3 \tag{118}$$

$$\frac{\partial\mathcal{L}}{\partial A^a_\mu} - \partial_\nu\frac{\partial\mathcal{L}}{\partial A^a_{\mu,\nu}} = 0, \quad \forall\mu = 0,1,2,3,\ a = 1,2,3. \tag{119}$$

These lead to the following equations for motion:

$$D_\mu D^\mu\phi^a + \lambda\phi^a\left(\phi^b\phi^b - v^2\right) = 0, \tag{120}$$

$$g\varepsilon^{abc}A^b_\nu F^{c,\nu}_\mu + g\varepsilon^{abc}D_\mu\phi^b\phi^c = \partial^\nu F^a_{\nu\mu}. \tag{121}$$

This last equation can be written in the following form:

$$D^\mu F^a_{\mu\nu} = gj^a_\nu \tag{122}$$

where

$$j^a_\mu = -\varepsilon^{abc}D_\mu\phi^b\phi^c \tag{123}$$

comes from the variation of the scalar part of the action with respect to A^a_μ.

We now assume a spherical symmetry for the solution of the fields ϕ^a and A^a_μ:

$$\begin{aligned} &\phi^a = vn^a h(r), \quad \partial_0\phi^a = 0, \\ &A^a_\mu = \frac{1}{gr}\varepsilon^{aij}n_j f(r), \quad A^a_0 = 0, \quad \partial_0 A^a_i = 0. \end{aligned} \tag{124}$$

Recalling that

$$\partial_i r = n_i, \quad \partial_i n_j = \frac{1}{r}\left(\delta_{ij} - n_i n_j\right), \tag{125}$$

we find by direct substitution into (120),(121) two second-order differential equation for the fonctions f and h:

$$r(rh'' + 2h') - 2h(f-1)^2 + \lambda v^2 r^2 h(1-h^2) = 0, \tag{126}$$
$$r^2 f'' - f(f-1)(f-2) = -g^2 v^2 r^2 h^2 (1-f). \tag{127}$$

For convenience, we can proceed to the following change of variable:

$$H(r) := rh(r) \quad \Rightarrow \quad H''(r) = rh''(r) + 2h'(r), \tag{128}$$
$$F(r) := f(r) - 1 \quad \Rightarrow \quad F''(r) = f''(r), \tag{129}$$

and by direct substitution we find the two equivalent equations:

$$r^2 H'' = 2HF^2 + \lambda v^2 H(H^2 - r^2), \tag{130}$$
$$r^2 F'' = F(F^2 - 1) - g v^2 H^2 F, \tag{131}$$

which correspond to the original equations found by 't Hooft and Polyakov.

A.1 Energy functionnal

The mass (or energy) of the monopole is one of the quantity which can be estimated analytically. We can show the the mass only depends upon the ratio of the two free parameters of the Lagrangian:

$$E \sim \frac{v}{g}. \tag{132}$$

Introducing a non-Minkowskian metric $g_{\mu\nu}$, the symmetric energy-momentum tensor writes:

$$\delta_{g_{\mu\nu}} S = \frac{1}{2} \int \mathrm{d}^4 x \sqrt{-g} \bar{T}^{\mu\nu} \delta g_{\mu\nu}. \tag{133}$$

We easily find that for the Lagrangian (115), the corresponding $\bar{T}^{\mu\nu}$ is

$$\bar{T}_{\mu\alpha} = -F_{\mu\nu} F_{\alpha}{}^{\nu} + \mathrm{D}_\mu \phi^a \mathrm{D}_\alpha \phi^a - \eta_{\mu\alpha} \mathcal{L}. \tag{134}$$

For a static configuration of the fields, the $\bar{T}_{00}$ component reduces to

$$\bar{T}_{00} = \frac{1}{2} F_{0i} F_{0i} + \frac{1}{4} F_{ij} F_{ij} + \frac{1}{2} \mathrm{D}_0 \phi^a \mathrm{D}_0 \phi^a + \frac{1}{2} \mathrm{D}_i \phi^a \mathrm{D}_i \phi^a + \frac{\lambda}{4} \left(\phi^a \phi^a - v^2 \right)^2 \tag{135}$$

Considering the 't Hooft Polyakov ansatz (124), the expression reduce even further, and the energy functionnal reads:

$$E = 4\pi \int_0^\infty r^2 \mathrm{d}r \left(\frac{1}{4} F_{ij} F_{ij} + \frac{1}{2} \mathrm{D}_i \phi^a \mathrm{D}_i \phi^a + \frac{\lambda}{4} \left(\phi^a \phi^a - v^2 \right)^2 \right). \tag{136}$$

In terms of f and h, it becomes:

$$E = \frac{4\pi}{g^2}\int_0^\infty \mathrm{d}r \left[f'^2 + \frac{f^2(f-2)^2}{2r^2} + \frac{v^2g^2}{2}r^2h'^2 \right.$$
$$\left. + v^2g^2h^2(1-f)^2 + \frac{\lambda}{4}v^4g^2r^2(h^2-1)^2 \right]. \quad (137)$$

Proceeding to the following change of variable:

$$f(r) = 1 - F(r); \quad h(r) = \frac{H(r)}{r}; \quad \xi = gvr. \quad (138)$$

The energy functional can be recast into

$$E = \frac{4\pi v}{g} C\left(\frac{\lambda}{g^2}\right) \quad (139)$$

We note that that the minimization of the energy functional (137) with respect to f and h lead to the same field equations as (126)-(127).

Given the numerical approximations for f and h found in previous section, we can estimate the energy in the following way:

$$\int_0^\infty \mathcal{E}(r, f, f', h, h')\mathrm{d}r \;\rightarrow\; \Delta\sum_{i=1}^{N}\mathcal{E}\left(r_i, f_i, \frac{f_{i+1}-fi-1}{\Delta}, h_i, \frac{h_{i+1}-h_{i-1}}{\Delta}\right) \quad (140)$$

where $\mathcal{E}$ is the energy density.

B Numerical integration of the equations of motion: the case of the Vortex

We assume that the field equations for the two degrees of freedom A and F are known, and given by

$$\begin{aligned} &-\frac{\mathrm{d}}{\mathrm{d}r}\left[r\frac{\mathrm{d}F}{\mathrm{d}r}\right] + \lambda v^2 r(F^2-1)F + \frac{F}{r}(A-1)^2 = 0, \\ &-\frac{\mathrm{d}}{\mathrm{d}r}\left[\frac{1}{r}\frac{\mathrm{d}A}{\mathrm{d}r}\right] - 2e^2v^2\frac{F^2(1-A)}{r} = 0 \end{aligned} \quad (141)$$

with the following asymptotic behaviour:

$$F(r) \to 1, \qquad A(r) \to 1, \qquad \text{as } r \to \infty, \quad (142)$$
$$F(r) \to 0, \qquad A(r) \to 0, \qquad \text{as } r \to 0. \quad (143)$$

We are looking for a numerical scheme which converge to a solution of (141) satisfiying these boundary conditions. Let's define for convenience the two auxiliary functions:

$$M(r, x, y) = \alpha r^2(y^2-1)y, \quad (144)$$
$$N(r, x, y) = \beta r y^2(1-x) \quad (145)$$

such that the system to solve reads:

$$\begin{cases} r^2F'' + rF' - M(r, A, F) = 0, \\ rA'' - A' + N(r, A, F) = 0. \end{cases} \tag{146}$$

The boundary condition at infinity is hard to implement, so in a first approximation, we choose a maximal radius R where both function A and F eventually reach 1. We hope that the result of the simulation will be a good approximation of the solution if R is sufficiently large.

We discretize the interval $[0, R]$ into N points uniformly distributed

$$r_i = ih, \quad h = \frac{R}{N+1} \quad \Longrightarrow \quad r_0 = 0,\ r_{N+1} = R, \tag{147}$$

and we write

$$a_i = A(r_i), \quad f_i = F(r_i). \tag{148}$$

The non-linear system (146) gives rise to the following finite differences scheme:

$$\frac{r_i^2}{h^2}(f_{i+1} - 2f_i + f_{i-1}) + \frac{r_i}{2h}(f_{i+1} - f_{i-1}) - M(r_i, a_i, f_i) = 0, \tag{149}$$

$$\frac{r_i}{h^2}(a_{i+1} - 2a_i + a_{i-1}) - \frac{1}{2h}(a_{i+1} - a_{i-1}) + N(r_i, a_i, f_i) = 0 \tag{150}$$

$\forall\ i = 1, \ldots, N$ with the boundary conditions:

$$a_0 = f_0 = 0, \quad a_{N+1} = f_{N+1} = 1. \tag{151}$$

In order to solve for the unknown a_i, f_i, let's write

$$x_i = \begin{cases} a_i, & \forall i = 1, \ldots, N \\ f_i, & \forall i = N+1, \ldots, 2N \end{cases} \tag{152}$$

and the numerical scheme becomes

$$\vec{g}(x_1, \ldots, x_{2N}) = \begin{bmatrix} g_1(x_1, \ldots, x_{2N}) \\ \vdots \\ g_{2N}(x_1, \ldots, x_{2N}) \end{bmatrix} = \begin{bmatrix} 0 \\ \vdots \\ 0 \end{bmatrix} \tag{153}$$

where

$$g_1(x) = \frac{r_1}{h^2}(x_2 - 2x_1) - \frac{1}{2h}x_2 + N(r_1, x_1, x_{N+1}), \tag{154}$$

$$g_N(x) = \frac{r_N}{h^2}(1 - 2x_N + x_{N-1}) - \frac{1}{2h}(1 - x_{N-1}) + N(r_N, x_N, x_{2N}), \tag{155}$$

$$g_{N+1}(x) = \frac{r_1^2}{h^2}(x_{N+2} - 2x_{N+1}) + \frac{r_1}{2h}x_{N+2} - M(r_1, x_1, x_{N+1}), \tag{156}$$

$$g_{2N}(x) = \frac{r_N^2}{h^2}(1 - 2x_{2N} + x_{2N-1}) + \frac{r_N}{2h}(1 - x_{2N-1}) - M(r_N, x_N, x_{2N}), \tag{157}$$

$$g_i(x) = \frac{r_i}{h^2}\left(x_{i+1} - 2x_i + x_{i-1}\right) - \frac{1}{2h}\left(x_{i+1} - x_{i-1}\right), \\ + N(r_i, x_i, x_{N+i}), \quad \forall i = 2, \ldots, N-1, \tag{158}$$

$$g_i(x) = \frac{r_{i-N}^2}{h^2}\left(x_{i+1} - 2x_i + x_{i-1}\right) - \frac{r_{i-N}}{2h}\left(x_{i+1} - x_{i-1}\right), \\ + M(r_{i-N}, x_{i-N}, x_i), \quad \forall i = N+2, \ldots, 2N-1. \tag{159}$$

We then use Newton-Raphson iteration to find the solution for the x_i's:

$$x^{i+1} = x^i - \frac{\vec{g}(x)}{J[\vec{g}]_x} \quad \Longleftrightarrow \quad J[\vec{g}]_x^{-1}\left(x^{i+1} - x^i\right) = \vec{g}(x) \tag{160}$$

where $J[\vec{g}]_x$ is the Jacobian matrix of $\vec{g}$ evaluated at x. The solution is given by $x = \lim_{i\to\infty} x^i$, and the convergence is faster if we choose cleverly the initial point x^0.

References

[1] S. Coleman. *Aspects of symmetry.* Cambridge University Press, 1988.

[2] V.A. Rubakov. *Classical theory of gauge fields.* Princeton University Press, 2002.

[3] Y.M. Shnir. *Magnetic monopoles.* Texts and monographs in physics. Springer, 2005.